# Continuous sub-monthly monitoring of global methane emissions from an ensemble Kalman filter at 2°×2.5° degrees using TROPOMI observations: application to interpretation of 2020–23 surge

Drew C. Pendergrass[1]*, Daniel J. Jacob[1], Nicholas Balasus[1], Lucas Estrada[1], Daniel J. Varon[1], Todd A. Mooring[1], James D. East[1], Elise Penn[2], and Hannah O. Nesser[3]

[1]School of Engineering and Applied Sciences, Harvard University, Cambridge, MA, USA. [2]Department of Earth and Planetary Sciences, Harvard University, Cambridge, MA, USA
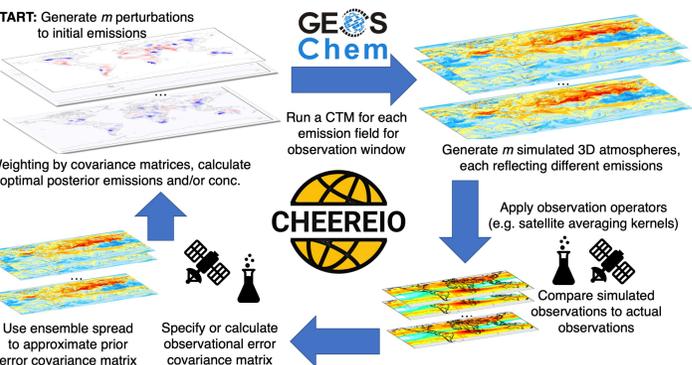[3]NASA Jet Propulsion Laboratory, Pasadena, CA, USA. *Drew Pendergrass is now a postdoc at Duke University.
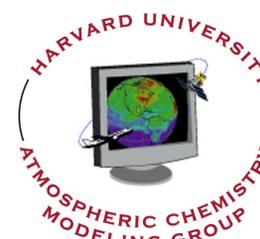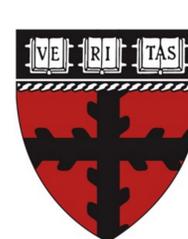
Abstract. We use 2019-2023 TROPOMI satellite observations of atmospheric methane to quantify global methane emissions at monthly $2°×2.5°$ resolution with a localized ensemble transform Kalman filter (LETKF) inversion, deriving monthly posterior estimates of emissions and year-to-year evolution. We apply two alternative wetland inventories (WetCHARTs and LPJ-wsl) as prior estimates. Our best posterior estimate of global emissions shows a surge from 560 Tg a^{-1} in 2019 to 587-592 Tg a^{-1} in 2020-2021 before declining to 572-570 Tg a^{-1} in 2022-2023. Posterior emissions reproduce the observed 2019-2023 trends in methane concentrations at NOAA surface sites and from TROPOMI across all major regions with minimal regional bias. Consistent with previous studies, we attribute the 2020-2021 methane surge to a 14 Tg a^{-1} increase in emissions from sub-Saharan Africa but find that previous attribution of this surge to anthropogenic sources (livestock) reflects errors in the assumed wetland spatial distribution. Correlation with GRACE-FO inundation data suggests that wetlands in South Sudan played a major role in the 2020-2021 surge but are poorly represented in wetland models. By contrast, boreal wetland emissions decreased over 2020-2023 consistent with drying measured by GRACE-FO. We find that the global seasonality of posterior emissions is driven by northern tropical wetlands and peaks in September, later than the July wetland model peak and consistent with GRACE-FO. We find no global seasonality in oil/gas emissions, but US fields show elevated cold season emissions that could reflect increased leakage.
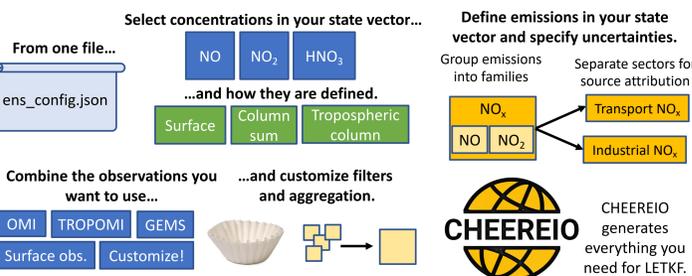
The LETKF algorithm

The **Localized Ensemble Transform Kalman Filter** (LETKF) is a Bayesian algorithm that can optimize emissions or concentrations of chemical species; LETKF uses an ensemble of chemical transport model (CTM) simulations, each driven by randomly perturbed emissions such that the CTMs represents the spread of atmospheric states that could result given emissions uncertainty. LETKF compares this suite of artificial atmospheres to real observations and uses the difference to calculate an update to the prior.

START: Generate *m* perturbations to initial emissions

Run a CTM for each emission field for observation window

Generate *m* simulated 3D atmospheres, each reflecting different emissions

Apply observation operators (e.g. satellite averaging kernels)

Weighting by covariance matrices, calculate optimal posterior emissions and/or conc.

Compare simulated observations to actual observations

Use ensemble spread to approximate prior error covariance matrix

Specify or calculate observational error covariance matrix

CHEEREIO data assimilation platform

CHEEREIO is a Python- and Shell-based wrapper for the GEOS-Chem CTM, automating the deployment of LETKF ensembles for a wide variety of observation types. In this study, we use CHEEREIO 1.3.0. CHEEREIO is open-source and freely available at **cheereio.seas.harvard.edu.**
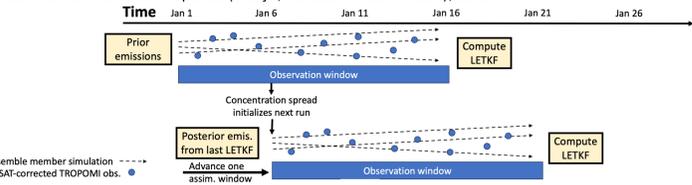
From one file...
ens_config.json

Select concentrations in your state vector...
NO   NO₂   HNO₃

...and how they are defined.
Surface   Column sum   Tropospheric column

Define emissions in your state vector and specify uncertainties.
Group emissions into families
NOₓ → NO   NO₂

Separate sectors for source attribution
NOₓ → Transport NOₓ   Industrial NOₓ

Combine the observations you want to use...
OMI   TROPOMI   GEMS   Surface obs.   Customize!

...and customize filters and aggregation.

CHEEREIO generates everything you need for LETKF.

LETKF modifications for methane

Lognormal errors prevent unphysical negative emissions, but imposing a lognormal distribution violates the LETKF equations. We solve this problem by sampling methane emissions scaling factors for each ensemble member according to a lognormal distribution centered on 1 (prior emissions inventory) and run GEOS-Chem, then for LETKF calculations we apply a log transform.

CTM simulations
LOG
Lognormal spread
EXP
Gaussian spread
LETKF
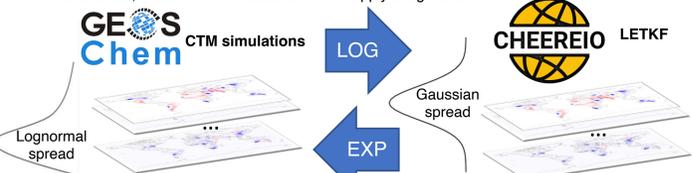
Run-in-place (RIP) assimilations recycle observations so that methane emissions estimates benefit from a longer observational record. With RIP, we calculate the LETKF assimilation update using a long period of observations (15 days, called the observation window), but then advance the assimilation window forward for a shorter period (5 days, the assimilation window), as shown below.

Time
Jan 1   Jan 6   Jan 11   Jan 16   Jan 21   Jan 26
Prior emissions
Observation window
Compute LETKF
Concentration spread initializes next run
Posterior emis. from last LETKF
Advance one assim. window
Observation window
Compute LETKF

Ensemble member simulation
GOSAT-corrected TROPOMI obs.

We built a **near-real-time system** for estimating **global methane emissions** with TROPOMI data, then applied it to 2018-2023 to study rapidly increasing atmospheric methane concentrations.
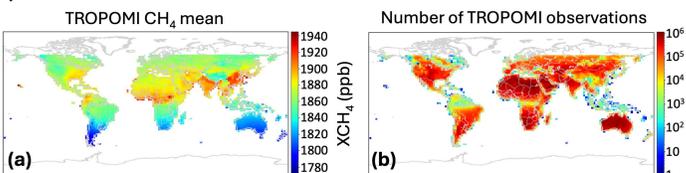
We attribute the 2020 **methane surge** to a 14 Tg a^{-1} increase in emissions from eastern Africa which has persisted.

Wetland models underestimate emissions in Africa, which has led previous work to incorrectly attribute the African surge to livestock.
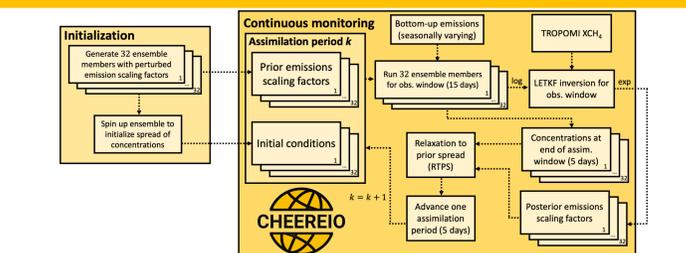
CHEEREIO website

Scan for more about using the CHEEREIO model for emissions quantification, and to read our preprint

Methane preprint

Emissions and TROPOMI observations

Prior fossil emissions are from GFEIv2 and other anthropogenic emissions are from EDGARv6, overwritten over the US, Mexico, and Canada by national inventories. Fires are from GFED4, termites from Fung et al. (1991), and seeps from Etiope et al. (2019). OH is prescribed and scaled to match methyl chloroform observations. **For wetland emissions, we run inversions for two separate inventories.** We use the high-performance WetCHARTs v1.3.1 mean and compare it to LPJ-wsl driven by MERRA-2. **We use TROPOMI observations bias-corrected with GOSAT.**
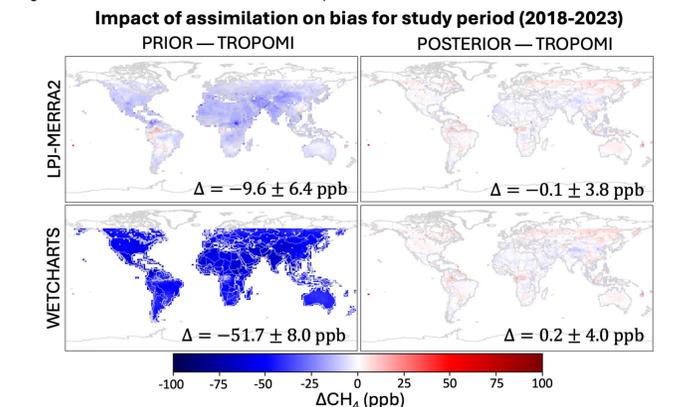
TROPOMI CH₄ mean
XCH₄ (ppb)
(a)

Number of TROPOMI observations
Count
(b)

Workflow for continuous monitoring

Initialization
Generate 32 ensemble members with perturbed emission scaling factors
Spin up ensemble to initialize spread of concentrations
Initial conditions

Continuous monitoring
Assimilation period *k*
Prior emissions scaling factors
Run 32 ensemble members for obs. window (15 days)
Bottom-up emissions (seasonally varying)
TROPOMI XCH₄
LETKF inversion for obs. window
Relaxation to prior (RTPS)
Concentrations at end of assim. window (5 days)
Advance one assimilation period (5 days)
Posterior emissions scaling factors
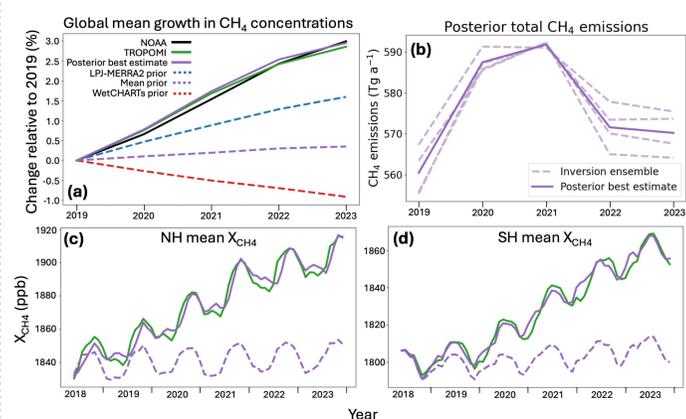*k = k + 1*

CHEEREIO

Post-assimilation spatial bias reduction

Below we show TROPOMI observations compared with GEOS-Chem simulations using either prior or posterior emissions for 2018-2023. ΔCH₄ denotes the difference between the simulation (with observation operators applied) and TROPOMI. Global mean bias and spatial standard deviation are given inset. Results are shown for wetlands prior estimates from either LPJ-MERRA2 or WetCHARTs.

Impact of assimilation on bias for study period (2018-2023)

PRIOR — TROPOMI | POSTERIOR — TROPOMI
LPJ-MERRA2: Δ = −9.6 ± 6.4 ppb | Δ = −0.1 ± 3.8 ppb
WETCHARTS: Δ = −51.7 ± 8.0 ppb | Δ = 0.2 ± 4.0 ppb

ΔCH₄ (ppb)
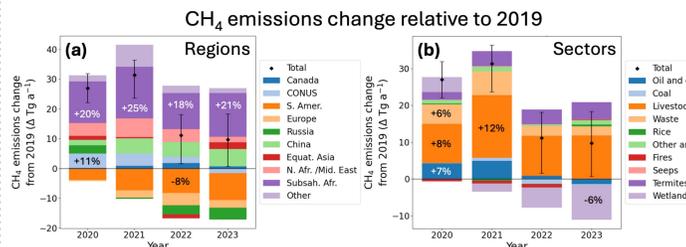-100 -75 -50 -25 0 25 50 75 100

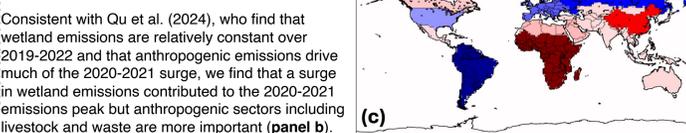
Interannual variability of methane emissions

Below we show relative growth in global annual mean methane concentrations over the study period including in NOAA mean concentrations from marine sites (**panel a**), showing our posterior result resolves the prior budget imbalance. In 2020 and 2021 we find that global methane emissions surged to 587 Tg a^{-1} and 592 Tg a^{-1} before declining to 572 Tg a^{-1} in 2022 and 570 Tg a^{-1} in 2023, consistent with the 2020 estimate of 581-627 Tg a^{-1} from Saunois et al. (2025) (**panel b**).

Global mean growth in CH₄ concentrations
(a)
NOAA
TROPOMI
Posterior best estimate
LPJ-wsl prior
Mean prior error
WetCHARTs prior

Posterior total CH₄ emissions
(b)
Inversion estimate
Posterior best estimate

NH mean XCH₄ (c)

SH mean XCH₄ (d)

To understand the drivers of our posterior emissions trends, we disaggregate our results by region and sector. We find a negative trend in South American emissions which we attribute to a decline in wetland emissions; this is consistent in sign with other top-down work finding wetland decreases.
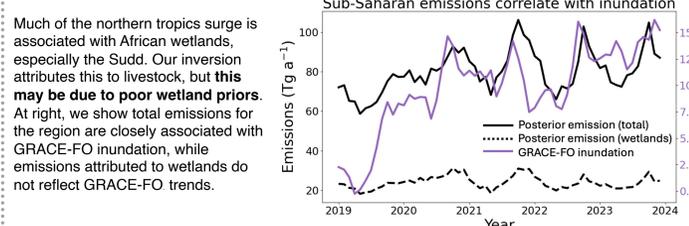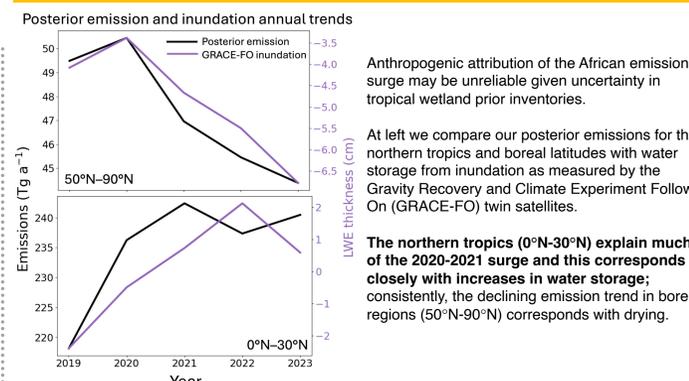
CH₄ emissions change relative to 2019

(a) Regions
Total, Canada, CONUS, S. Amer., Europe, Russia, China, Equat. Asia, N. Afr./Mid. East, Subsah. Afr., Other
+20%, +25%, +18%, +21%, +11%, -8%

(b) Sectors
Total, Oil and gas, Coal, Livestock, Waste, Rice, Other anthro., Fires, Seeps, Termites, Wetlands
+6%, +12%, +8%, +7%, -6%

We attribute the 2020 methane surge to a 14 Tg a^{-1} increase in emissions from sub-Saharan Africa.

Consistent with Qu et al. (2024), who find that wetland emissions are relatively constant over 2019-2022 and that anthropogenic emissions drive much of the 2020-2021 surge, we find that a surge in wetland emissions contributed to the 2020-2021 emissions peak but anthropogenic sectors including livestock and waste are more important (**panel b**).

In the right column, we analyze the reliability of the prior inventories informing this source attribution.

2019-23 posterior emissions trend
(c)
CH₄ emissions trend (Tg a^{-1})
-2 -1 0 1 2

Drivers of methane trends and seasonality

Posterior emission and inundation annual trends
Posterior emission
GRACE-FO inundation
50°N–90°N
0°N–30°N

Anthropogenic attribution of the African emission surge may be unreliable given uncertainty in tropical wetland prior inventories.

At left we compare our posterior emissions for the northern tropics and boreal latitudes with water storage from inundation as measured by the Gravity Recovery and Climate Experiment Follow-On (GRACE-FO) twin satellites.

The northern tropics (0°N-30°N) explain much of the 2020-2021 surge and this corresponds closely with increases in water storage; consistently, the declining emission trend in boreal regions (50°N-90°N) corresponds with drying.

Much of the northern tropics surge is associated with African wetlands, especially the Sudd. Our inversion attributes this to livestock, but **this may be due to poor wetland priors**. At right, we show total emissions for the region are closely associated with GRACE-FO inundation, while emissions attributed to livestock do not reflect GRACE-FO trends.

Sub-Saharan emissions correlate with inundation
Posterior emission (total)
Posterior emission (wetlands)
GRACE-FO inundation

Below we show the global seasonal cycle of posterior methane emissions for 2021. Unlike the prior estimates which show a July-August peak in the northern hemisphere (**panel a**), we find a sharp September peak driven by tropical emissions which strongly influences global seasonality (**panel b**). **Panel c** shows that the peak of northern tropical emissions corresponds with the peak of mean GRACE-FO water storage data, and occurs later in the year than implied by prior inventories.

Emission seasonality by NH sector (2021)
(a)
Posterior total
Prior (LPJ-MERRA2)
Prior (WetCHARTs)
Oil and gas, Coal, Livestock, Waste, Rice, Other anthro., Fires, Seeps, Termites, Wetlands

Emission seasonality by latitude (2021)
(b)
Posterior total
Prior (LPJ-MERRA2)
Prior (WetCHARTs)
90°S-50°S, 50°S-30°S, 30°S-10°S, 10°S-10°N, 10°N-30°N, 30°N-50°N, 50°N-90°N

Northern tropics (0°N–30°N) emissions and inundation seasonality (2021)
(c)
Posterior emission
Prior emission (LPJ-MERRA2)
Prior emission (WetCHARTs)
GRACE-FO inundation

We observe methane emission seasonality in some oil and gas production basins especially in the US. At right we show best-estimate posterior fossil fuel emissions in cold months minus warm months, with many areas showing elevated cold season emissions including several major US basins, Hassi R'Mel field (Algeria), Sirte basin (Libya), and West Karun basin (Iran).

Cold minus warm season fossil emissions
(a)
Uinta, Permian (b), Hassi R'Mel, Sirte (c)
ΔMg km^{-2}
-10.0 -7.5 -5.0 -2.5 0 2.5 5.0 7.5 10.0

Acknowledgements, contact, and links

Scan for this preprint on methane

Scan for 2023 CHEEREIO GMD paper